

On the Significance of Correlations Among Neuronal Spike Trains

G. Palm¹, A. M. H. J. Aertsen¹, and G. L. Gerstein²

¹ Max-Planck-Institut für Biologische Kybernetik, Spemannstrasse 38, D-7400 Tübingen, Federal Republic of Germany

² Department of Physiology, University of Pennsylvania, Philadelphia, PA 19104-6085, USA

Abstract. We consider several measures for the correlation of firing activity among different neurons, based on coincidence counts obtained from simultaneously recorded spike trains. We obtain explicit formulae for the probability distributions of these measures. This allows an exact, quantitative assessment of significance levels, and thus a comparison of data obtained in different experimental paradigms. In particular it is possible to compare stimulus-locked, and therefore time dependent correlations for different stimuli and also for different times relative to stimulus onset. This allows to separate purely stimulus-induced correlation from intrinsic interneuronal correlation. It further allows investigation of the dynamic characteristics of the interneuronal correlation. For the display of significance levels or the corresponding probabilities we propose a logarithmic measure, called “surprise”.

Introduction

In the last years there has been an increasing interest in multi-unit recordings of neuronal activity, i.e. simultaneous and separable observation of up to some 30 spike trains. Several groups have developed multi-electrode set-ups for this purpose, using various recording technologies (Gerstein et al. 1983; Krüger 1983; Grinvald 1985).

The main advantage of multi-unit recordings in comparison to single-unit recordings is the opportunity to study the interactions among several neurons as they react to a stimulus, rather than just the isolated reaction of each single neuron to the stimulus. The most important quantitative measure in extracellular recordings for the strength of interaction between neurons is the correlation of firing activity. Neuronal

spikes are regarded as stereotypic events; correlation thus simplifies to counting near-coincident events. The results are displayed as correlograms.

Coincidence of firing and correlation analysis of multi-unit data has been discussed since the 1960s (Perkel et al. 1967; Gerstein and Perkel 1969, 1972; Perkel et al. 1975; Glaser and Ruchkin 1976), and there are well-established procedures for interpretation of such calculations (Abeles 1982; Gerstein et al. 1983; Krüger 1983). When the results of several different experiments are to be compared, it is essential to have procedures for correction and normalization of the calculations. In particular it is necessary to compensate for variations in individual neuron firing rates, since these directly influence the observed near-coincidence rates. These variations of individual firing rates are conveniently measured with the Peri-Stimulus-Time (PST) histogram. For ordinary cross-correlation the usual procedure to compensate for direct stimulus effects on firing rates is to subtract a so-called “shift predictor” (or “PST histogram based predictor”) from the raw correlogram. Residuals are then interpreted as indication of “effective connectivity”. More complex normalizations are appropriate for the Joint PST histogram, a particular stimulus-locked temporal decomposition of the correlogram (Gerstein and Perkel 1969, 1972): besides subtracting a PST histogram based predictor, the matrix is scaled, bin by bin, by the product of the variances of the two PST histograms (Aertsen et al. 1988).

The kind of normalization procedures just described offers a measure of deviation from a null hypothesis; the size of such deviations is a measure of their significance. In our case, where we want to demonstrate neuronal interaction, the appropriate null hypothesis is (1) two completely independent neurons that (2) respond to the stimulus exactly as shown by the two experimentally observed PST histograms. More specifically: significance for positive

deviation from the null hypothesis is determined from the probability of having a near-coincidence count that is at least as high as the observed count, and significance for negative deviation is determined from the probability of having a near-coincidence count that is at most as high as the observed count.

In this paper we will show that these probabilities for the Joint PST histogram (JPSTH) can be expressed in closed form. These results also allow explicit calculation of the distributions of correlation values after application of any of the various types of normalization that have been proposed. These calculations therefore provide a sound basis for the evaluation of significance in correlation measurements and, hence, for the significance of their interpretation. Procedures for the analysis of firing correlations in multi-neuron recordings have benefited from these developments. Recent work along these lines is producing evidence for dynamic cooperativity as an emergent property of neuronal assembly organization in the brain (Gerstein 1987; Aertsen et al. 1988; Gerstein et al. 1988).

1 Calculations of the Probability Densities of Coincidence Counts

The experimental design is usually the following: A certain stimulus is repeatedly presented for a number of times, $i=1, \dots, n$. During each presentation of the stimulus, spike trains are recorded from two neurons.

Our calculations are based on the following set of assumptions:

1. Spikes are considered as identical *events* for which only the time of occurrence is relevant.
2. We impose discrete *time-bins*, such that each spike train is transformed into a 0–1 *process*. This requires that the time-bin be so small that there will be *at most one spike* in each bin. We will let the time marker associated with each stimulus presentation fall directly onto one such bin.
3. Firing activity during different (repeated) stimulus presentations is statistically indistinguishable. This means there are no long term nonstationarities in the data.

The recording time T per stimulus presentation is divided into J time-bins B_1, \dots, B_J . Thus the total recording time $n \cdot T$ is divided into $n \cdot J$ bins, and B^i_j denotes the j -th bin during the i -th stimulus presentation (see Fig. 1). The activity of each neuron, averaged over the many stimulus presentations, is given by the corresponding PST histogram; counts are generally different from bin to bin and reflect the stimulus-locked firing rate modulation for that particular neuron.

Assumption 2 has the following mathematical consequence: the numbers of spikes X^i_j observed in the

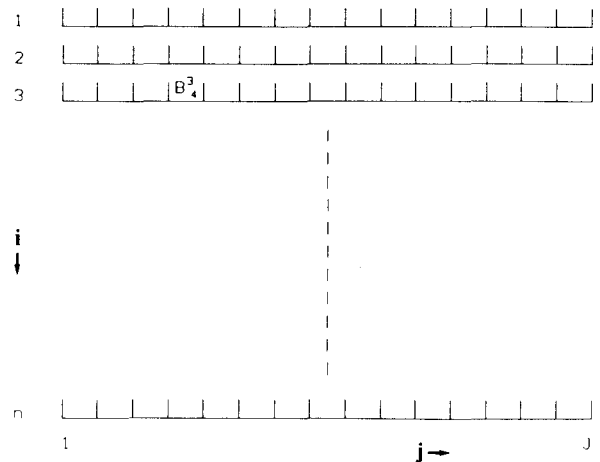


Fig. 1. Scheme of time binning, applied to spike trains, recorded during successive stimulus presentations. Further explanation in text

bins B^i_j are random variables with values in $\{0, 1\}$. Assumption 3 means that the conditions at a particular bin (lower index j) are the same for all successive stimulus presentations (upper index i): the variables X^1_j, \dots, X^n_j are independent and identically distributed (i.i.d.).

The mathematical problem can now be formulated as follows: We want to analyze (delayed) coincidence counts between two such variables (which usually would be from two different, simultaneously recorded neurons). We will use shorthand notation X and Y to indicate the two variables at the selected bins; from here on we will implicitly refer to this particular bin selection. Over the sequence of stimulus presentations, we then have two sequences of random variables X^1, \dots, X^n and Y^1, \dots, Y^n , both independent and identically distributed in $\{0, 1\}$.

The null hypothesis for the following calculations is that X^i and Y^i are independent.

1.1 Calculation in Terms of Single Unit Firing Probabilities

The distribution of X^i is determined by the firing probability $p = \text{pr}[X^i = 1]$; similarly the distribution of Y^i is given by the probability $q = \text{pr}[Y^i = 1]$. In this subsection we assume that these two probabilities are given.

Note that normally these probabilities are not given, and the best one can do is to assume that they are identical to the average spike frequencies, evaluated in the appropriate bins, of the two neurons under the stimulation used in the experiment. This case is treated more appropriately in the next subsection (1.2).

Given p and q it is straightforward to calculate both the probability density and the (cumulative) distribution of the coincidence count. First we note that for the specific selected bins, $X = \sum_{i=1}^n X^i$ is the spike count for the X^i -sequence, $Y = \sum_{i=1}^n Y^i$ is the spike count for the Y^i -sequence, and $Z = \sum_{i=1}^n X^i \cdot Y^i$ equals the coincidence count. For the probability density of the coincidence count we may write:

$$\text{pr}[Z=m] = \sum_{k=1}^n \text{pr}[Z=m | X=k] \cdot \text{pr}[X=k]. \quad (1)$$

These conditional probabilities can be determined as follows: if $X=k$ we may as well assume that $X^1, \dots, X^k=1$ and $X^{k+1}, \dots, X^n=0$, and therefore that the coincidence count Z equals $\sum_{i=1}^k Y^i$ and is binomially distributed.

Thus we may write:

$$\text{pr}[Z=m | X=k] = b(m; k, q) = \binom{k}{m} \cdot q^m (1-q)^{k-m} \quad (2)$$

and

$$\text{pr}[Z=m] = \sum_{k=1}^n b(m; k, q) \cdot b(k; n, p). \quad (3)$$

We can rewrite the probability density (3) into the corresponding cumulative distribution, simply by appropriate summation.

Equation (3) can be easily evaluated; some examples of the cumulative distribution for different values of n , p , and q are shown in Fig. 2a. Clearly every value of Z between 0 and n occurs with non-zero probability, but in fact the probability that Z is larger than $n \cdot p$ or $n \cdot q$, is very low and therefore in Fig. 2a we only displayed the curves for this lower range of Z -values.

Next we calculate the expectation of Z and Z^2 , and the variance of Z :

$$\begin{aligned} E[Z] &= \sum_{k=1}^n E(Z | X=k) \cdot \text{pr}[X=k] \\ &= \sum_{k=1}^n q \cdot k \cdot \text{pr}[X=k] \\ &= q \cdot E[X] = n \cdot p \cdot q, \end{aligned} \quad (4)$$

$$\begin{aligned} E[Z^2] &= \sum_{k=1}^n E(Z^2 | X=k) \cdot \text{pr}[X=k] \\ &= \sum_{k=1}^n (kq + k(k-1)q^2) \cdot \text{pr}[X=k] \\ &= (q - q^2)E[X] + q^2 E[X^2] \\ &= q(1-q) \cdot n \cdot p + q^2(np + n(n-1)p^2) \\ &= n^2 p^2 q^2 + n(pq - p^2 q^2), \end{aligned} \quad (5)$$

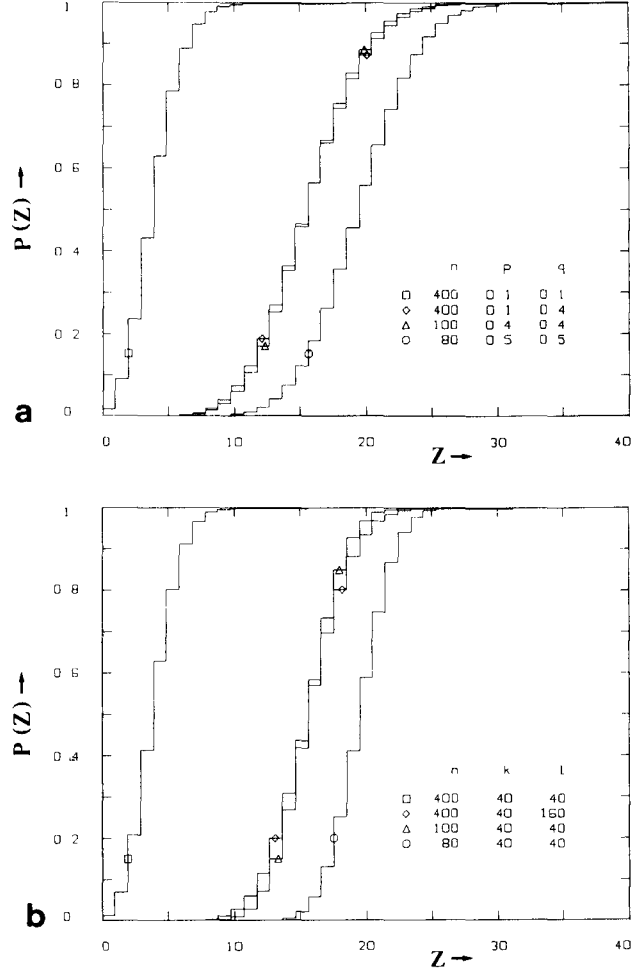


Fig. 2a and b. Examples of cumulative distribution function of coincidence count Z for different numbers of stimulus presentations n and neuronal firing rates. **a** Calculation in terms of single unit firing probabilities p and q . **b** Calculation in terms of observed single unit spike counts k and l

and

$$\text{Var}(Z) = n(pq - p^2 q^2). \quad (6)$$

Actually, the probability given in (3) is not really relevant in the typical experimental situation, because there one does not know the underlying probabilities p and q . One usually knows only the actual spike counts in the selected bins. If additional information were available, it could be used to make reasonable estimates for p and q for use in the above equations. For example, if one may assume that the firing probability is about the same in neighbouring bins, it is reasonable to average over these bins to determine p and q . It may sometimes be of interest to use this kind of neighbourhood sampling, especially for the variability correction that is mentioned in the introduction. Another example of additional information might be the availability of a model for the firing probabilities.

1.2 Calculation from the Observed Single Unit Spike Counts

In the usual experimental case, we do not have additional information; it is only possible to make the estimates in terms of the counts themselves, i.e. by using as estimates $p = k/n$ and $q = l/n$. In this case one might as well work directly in terms of the counts, rather than indirectly in terms of functions of these same counts.

Thus the appropriate mathematical description of the usual situation is that the experimenter just has four counts available: $X = k$, $Y = l$, and $Z = m$ and the number of stimulus presentations n . From these four numbers k, l, m, n we want to know the significance of the coincidence count m , given the firing counts of the two neurons are k and l during the n stimulus presentations. In this case one has to calculate the distribution of Z under the condition that $X = k$ and $Y = l$.

Without loss of generality we can assume that $k \leq l$ and, additionally, that $Y^1, \dots, Y^l = 1$ and $Y^{l+1}, \dots, Y^n = 0$.

The probability $\text{pr}[Z = m | X = k \text{ and } Y = l]$ is the probability that m out of the $k X^i$ -s which are 1, occur before l , while the remaining $k - m$ of these $k X^i$ -s occur after l , i.e.

$$\text{pr}[Z = m | X = k \text{ and } Y = l] = \frac{\binom{l}{m} \cdot \binom{n-l}{k-m}}{\binom{n}{k}}. \quad (7)$$

In this expression it may happen that $n - l < k - m$, i.e. $n + m < k + l$; in that case we define

$$\binom{n-l}{k-m} = 0.$$

Expression (7) can be easily evaluated (see Fig. 2b for some examples of the cumulative distribution for different values of n, k , and l ; observe the similarity to Fig. 2a) and we can again calculate the mean and the variance of the corresponding distribution:

$$E(Z | X = k, Y = l) = \frac{k \cdot l}{n}, \quad (8)$$

$$E(Z^2 | X = k, Y = l) = \frac{k \cdot l(k-1)(l-1)}{n \cdot (n-1)} + \frac{k \cdot l}{n}, \quad (9)$$

and

$$\text{Var}(Z | X = k, Y = l) = 1/(n-1) \cdot k(1-k/n) \cdot l(1-l/n). \quad (10)$$

If we express this in terms of rates, $\kappa = k/n$ and $\lambda = l/n$, we may write

$$E(Z | X = k, Y = l) = n \cdot \kappa \cdot \lambda \quad (11)$$

and

$$\text{Var}(Z | X = k, Y = l) = n^2/(n-1) \cdot \kappa(1-\kappa) \cdot \lambda(1-\lambda). \quad (12)$$

2 Normalized Correlations

Given the counts $X = k$, $Y = l$, $Z = m$ and n as in the preceding section, several formulae have been used in the literature to normalize the coincidence counts (e.g. Kuznetsov and Stratonovich 1956; Gerstein and Perkel 1969, 1972; Habib and Sen 1985; Boogaard et al. 1986; Aertsen et al. 1987, 1988). The aim of such normalization is to allow interpretation within an experiment and comparison across experiments.

Among these normalization procedures the earliest idea was the so-called "shift or (shuffle) predictor" (Perkel et al. 1967; Gerstein and Perkel 1969, 1972): take any permutation of stimulus presentations $\Pi: \{1, \dots, n\} \rightarrow \{1, \dots, n\}$ and form the shuffled correlation $Z'_\Pi = \sum X^i Y^{\Pi(i)}$. Now one can consider the difference $D'_\Pi = Z - Z'_\Pi$ as a correlation that is corrected for pure stimulus effects. Since this procedure depends on the choice of the permutation Π , an obvious idea is to average this over all possible permutations Π . This leads to the expression

$$\begin{aligned} D' &= \frac{1}{n!} \cdot \sum_{\Pi} D'_\Pi = Z - \frac{1}{n!} \cdot \sum_{\Pi} \sum_{i=1}^n X^i Y^{\Pi(i)} \\ &= Z - \sum_{i=1}^n X^i Y = Z - (X \cdot Y)/n. \end{aligned} \quad (13)$$

In other words: the average over the set of all possible "shift (or shuffle) predictors" is equivalent to a predictor based on the cross product of the PST histograms.

In the following we simply list the various expressions which have been suggested and which will be considered here, also including one new suggestion (e).

(a) Subtraction of the expected coincidence [cf. (13)]:

$$D = Z - (X \cdot Y)/n. \quad (14)$$

(b) Division by the expected coincidence:

$$Q = Z \cdot n / (X \cdot Y). \quad (15)$$

(c) Subtraction of the expected coincidence, followed by division by the expected coincidence:

$$R = D \cdot n / (X \cdot Y). \quad (16)$$

(d) Subtraction of the expected coincidence, followed by division by the product of the estimated standard deviations of X and Y . This leads to a correlation coefficient:

$$C = D / \{X(1-X/n) \cdot Y(1-Y/n)\}^{1/2}. \quad (17)$$

In the quantity C , the difference D has been normalised to values in the range $[-1, 1]$.

(e) Subtraction of the expected coincidence, followed by division by the conditional standard deviation of Z (given $X = k$ and $Y = l$) as determined in (10):

$$\begin{aligned} S &= \sqrt{(n-1)} \cdot D / \{X(1-X/n) \cdot Y(1-Y/n)\}^{1/2} \\ &= \sqrt{(n-1)} \cdot C. \end{aligned} \quad (18)$$

S is essentially the standardization of Z .

Note that, like the various counts X , Y , and Z , these normalized correlations are stochastic variables. In the following we will consider their distribution and first and second moments.

2.1 Calculation in Terms of Single Unit Firing Probabilities

Given the firing probabilities p and q as in Sect. 1.1, it turns out to be a hard mathematical problem to determine the distribution or moments of these statistics. In fact, only for D were we able to determine the distribution in closed form.

Analogously to (1) we have

$$\text{pr}[D=d] = \sum_{k=1}^n \text{pr}[D=d | X=k] \cdot \text{pr}[X=k]. \quad (19)$$

If $X=k$, we may again assume that $X^1, \dots, X^k=1$ and $X^{k+1}, \dots, X^n=0$. Thus for $X=k$ we have

$$\begin{aligned} D &= Z - X \cdot Y/n = \sum_{i=1}^k Y^i - (k/n) \cdot \sum_{i=1}^n Y^i \\ &= (1-k/n) \cdot \sum_{i=1}^k Y^i - (k/n) \cdot \sum_{i=k+1}^n Y^i \\ &= (1-k/n) \cdot S_1 - (k/n) \cdot S_2. \end{aligned} \quad (20)$$

Under the condition that $X=k$, the variable D is apparently a linear combination of two independent, binomially distributed random variables S_1 and S_2 , where the distribution of S_1 is $b(s_1; k, q)$ and that of S_2 is $b(s_2; n-k, q)$. From these distributions one can compute $\text{pr}[D=d | X=k]$, and from (19) we then obtain $\text{pr}[D=d]$. Some examples of the cumulative distribution of D are shown in Fig. 3, which will be discussed in Sect. 3.

2.2 Calculation from the Observed Single Unit Spike Counts

In the case where we work with the conditional probabilities given that $X=k$ and $Y=l$ as in Sect. 1.2, we can easily determine the probability density of any of the above correlation measures. Let us consider, for example, the correlation coefficient C . Under the given conditions for the individual spike counts $X=k$ and $Y=l$, the only remaining stochastic variable in the

value of C is the coincidence count $Z=m$. Hence, we may simply write:

$$\begin{aligned} \text{pr} \left[C = \frac{m - kl/n}{\{k(1-k/n) \cdot l(1-l/n)\}^{1/2}} \middle| X=k \text{ and } Y=l \right] \\ = \text{pr}[Z=m | X=k \text{ and } Y=l]. \end{aligned} \quad (21)$$

Similar reasoning can be used to obtain probability densities for the other correlation measures.

Equations (7)–(12) also lead us to the expectation and variance of each of the above measures under the condition that $X=k$ and $Y=l$. In the following equations we will no longer explicitly indicate this condition.

$$(a) \ E(D)=0; \quad \text{Var}(D)=\text{Var}(Z), \quad (22)$$

$$(b) \ E(Q)=1; \quad \text{Var}(Q)=(1-\kappa)(1-\lambda)/(\kappa\lambda(n-1)), \quad (23)$$

$$(c) \ E(R)=0; \quad \text{Var}(R)=\text{Var}(Q), \quad (24)$$

$$(d) \ E(C)=0; \quad \text{Var}(C)=1/(n-1), \quad (25)$$

$$(e) \ E(S)=0; \quad \text{Var}(S)=1. \quad (26)$$

For large n , the measures C , Q , and R have decreasing variance with increasing n . The correlation coefficient C has the smallest variance as long as κ and λ are below $1/2$ (which is the usual case for physiological data). The standardized coincidence count S has to have variance 1 by definition: it therefore must have values outside the range $[-1, 1]$. Z itself and of course D are the only coincidence measures whose variance increases with n .

2.3 Significance of Experimentally Observed Correlations

Having derived explicit expressions for the distributions of the various normalized correlation measures, we can now address the significance of finding a particular value for any of these measures. Here we can use the ordinary approach to this problem. The significance of downward deviation (negative correlation measure) is the probability of finding that value or a lower one; this can simply be read off the lower end of the plotted corresponding cumulative distribution function. The significance of an upward deviation is the probability of finding that value or a higher one; this can simply be read off the upper end of the plotted cumulative distribution function.

3 Comparison to the Gaussian Distribution

In this and the following sections we will concentrate the discussion on the expressions in terms of observed single unit spike counts (as in Sects. 1.2 and 2.2), since only in this case can we explicitly calculate all relevant

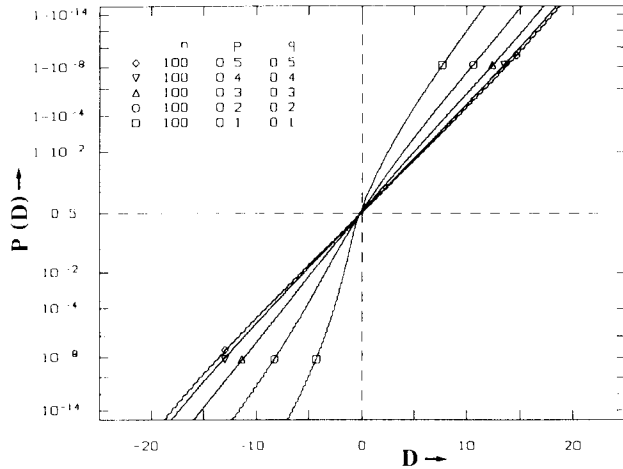


Fig. 3. Examples of cumulative distribution function of correlation measure D for constant number of stimulus presentations n and different single unit firing probabilities $p=q$. The cumulative distribution function $P(D)$ is plotted on Gaussian probability paper

distributions without resorting to Gaussian approximations in the first place. Also this case is probably the experimentally more relevant one. Of course, for large n , all the measures of correlation will be approximately normally distributed. To the extent that such an approximation is valid, the normal distributions will then be fully characterized by the corresponding mean and variance, as given in (22)–(26). Such mean and variance can then be used directly for significance statements.

In the usual experimental situation, however, the number n of stimulus presentations will not be very large – values of $n \leq 100$ are a common case. Therefore it is appropriate to study the departure from normality of the various correlation measures as a function of the parameters n , k , and l (or n , p , and q). This can be done by examining the exact distribution of the correlation measures on Gaussian probability paper, i.e. transformed by the inverse of the cumulative normal distribution function (as in Figs. 3 and 4). In such a plot the normal distribution appears as a straight line, going through the origin.

The most commonly used measure of correlation is the correlation coefficient C , referred to as “cross-correlation surface” by Habib and Sen (1985) and as “normalized Joint Peri-Stimulus Time Histogram” in Aertsen et al. (1988). For investigation of the departure from Gaussian, however, it is more convenient to work with the standardized correlation S (as in Fig. 4), because in such a plot all curves should have the same slope, independent of all parameters, in particular of n . When we worked with the firing probabilities p and q , we were unable to calculate the distribution of S ;

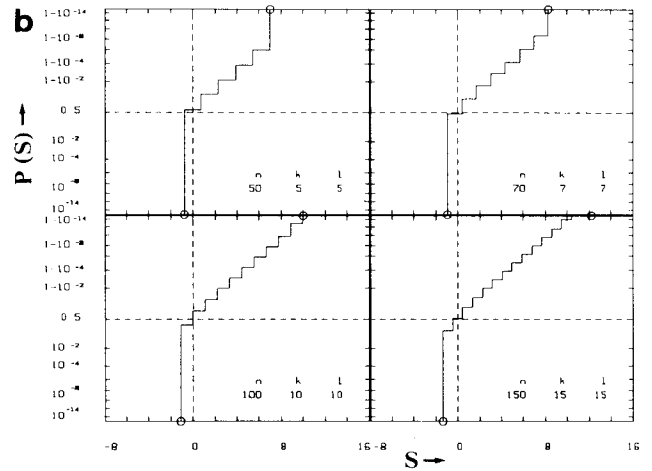
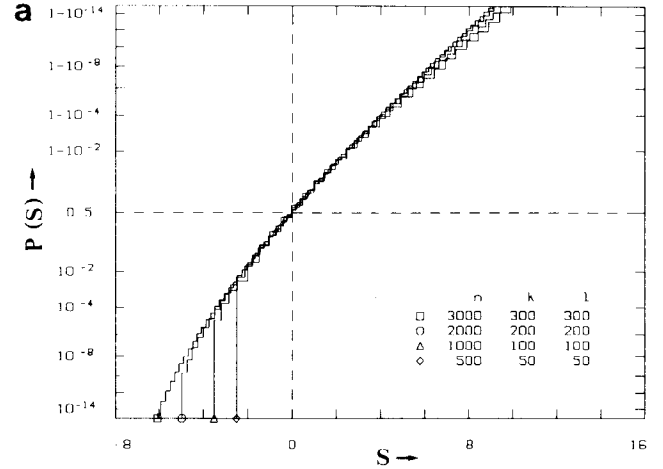


Fig. 4a and b. Examples of cumulative distribution function of standardized correlation S for different numbers of stimulus presentations n and constant spike counts per presentation $\kappa = \lambda$. The cumulative distribution function $P(S)$ is plotted on Gaussian probability paper. **a** Superposition of four $P(S)$ -curves for large n . **b** Separate plots of four $P(S)$ -curves for smaller n

therefore for this case we display the distribution of D (Fig. 3). In such a plot the curves will have different slope for different parameters.

Let us start with the discussion of the expressions in terms of single unit firing probabilities p and q (cf. Sects. 1.1 and 2.1). Figure 3 shows some cumulative distributions of D for different values of $p=q$ and constant $n=100$, plotted on Gaussian probability paper. The frame in Figs. 3 (and 4) has been set to cover the range of cumulative probability values between 10^{-15} and $1 - 10^{-15}$, corresponding to significance levels of up to 10^{-15} . As should be expected, the curves for higher values of p have a lower overall slope and are closer to a straight line. For $p=0.5$ the curve is symmetric around $D=0$, and virtually indistinguishable from a straight line (i.e. from a Gaussian distribution). For lower

values of p , the curves becomes increasingly asymmetric and skewed, with higher average slope for negative D . Altogether, the deviations from the Gaussian distribution appear to be rather small for the relatively low value of $n=100$.

We now turn to the expressions in terms of observed single unit spike counts k and l (cf. Sects. 1.2 and 2.2), which in general show a more pronounced deviation from the Gaussian. Figure 4 shows some cumulative distributions for the standardized correlation S as plotted on Gaussian probability paper. Note that in this figure we varied n , while keeping the fractions κ and λ constant (0.1). Figure 4a shows a superposition of four curves for $n=500, 1000, 2000$, and 3000 ; Figure 4b shows four separate plots of the cases $n=50, 70, 100$, and 150 . Interestingly, the curves in Fig. 4a (i.e. for large n) can be reasonably well approximated by a straight line. There is, however, always a slight curvature to the right: decreasing slope for increasing S . As was to be expected, the departure from Gaussian increases for decreasing n . They are worst at the smallest, but experimentally realistic values of n used in Fig. 4b.

The probability of zero coincidences is given by the size of the first step in the cumulative distribution staircase plot; the probability of maximal number of coincidences is given by the size of the last step. In each case the position of the first step along the S -coordinate is indicated by a symbol. Observe that these positions, as well as the corresponding probabilities, do not reach down to the lower left corner of the graph, especially for smaller n . The position of the last step along the S -coordinate is indicated by a symbol for small n (Fig. 4b), for larger n (Fig. 4a) this last step is well beyond the displayed S -range. The last step in the plot is always much smaller than the first step; in fact it is virtually zero, with the exception of the cases $n=50$ and $n=70$. Furthermore the range of positive S -values is always considerably larger than the range of negative S -values (note the asymmetry of the S -axis). This means that the range of attainable S -values, as well as probability values and, consequently, significance values, for negative interaction is considerably smaller than for positive interaction. In particular, very low probabilities, i.e. very high levels of significance for negative interaction cannot be reached, except for unrealistically large values of n . Note that in the more realistic cases shown in Fig. 4b, cumulative probabilities smaller than 0.5 or negative S -values (i.e. inhibition) can only be found in the extreme case of zero coincidences.

The practical consequence of this positive-negative asymmetry can be formulated in two ways. For a given number of stimulus presentations n , there is a severe limitation to the attainable deviation in the negative

direction, and hence to the significance that can be attained for negative interaction (“inhibition”); there is no severe limitation for deviations in the positive direction (“excitation”). Conversely, attaining a required level of significance requires a higher value of n (i.e. more stimulus presentations) for deviations in the negative direction than for deviations in the positive direction. These consequences of the asymmetry have already been noted in cross-correlation analysis of multi-neuron data: for neurons firing at typical rates, inhibition is much harder to detect than excitation (Aertsen and Gerstein 1985).

Figure 4 and the above comments are appropriate for the case of typical parameter values k and l which are less than $n/2$. For k and l around $n/2$ the curves become more symmetric and actually quite similar to a normal distribution. This suggests another strategy for enhancing detectability of inhibition: increase the firing rates of the neurons by some means (e.g. by sensory or pharmacological stimulation). For k and l larger than $n/2$, the plots now become curved in the opposite direction, and the asymmetry reverses: it is now harder to attain significance for positive interaction than for negative interaction.

4 Maximum and Minimum of the Distribution of C , D or S

A simple way of quantifying the difference in sensitivity of the correlation measures for “excitation” (positive correlation) and for “inhibition” (negative correlation) is to calculate their *range*. Let us consider, for example, the correlation coefficient C . Theoretically, C values are allowed to cover the range $[-1, 1]$. For any specific set of numbers k, l, m, n , however, the positive and negative ranges that are actually covered will in general not be the same. For k and l smaller than $n/2$ (the usual physiological case), we show below that the positive range is larger than the negative range. For k and l larger than $n/2$, the relationship between positive and negative ranges is reversed.

Let $\text{Max}(C)$ and $\text{Min}(C)$ denote the maximum and minimum of C . The ratio $a = |\text{Max}(C)/\text{Min}(C)|$ can then be taken as a measure for the asymmetry of the positive and negative ranges. From the known range of the coincidence count Z , the asymmetry a for measure C can be easily calculated. Furthermore, the asymmetries for all measures C , D , R , and S are identical, because these measures differ only in the denominator. Since the range of D is the easiest to calculate, we shall in the following determine a from

$$a = |\text{Max}(D)/\text{Min}(D)|. \quad (27)$$

For counts k and l such that $k+l \leq n$, it is clear that Z ranges from 0 to the minimum of k and l . For $k+l > n$ there must be some coincidences: Z is at least $k+l-n$.

A more general formulation can be obtained by introducing the notation $\text{Inf}(x, y)$ for the smaller of x and y , and $\text{Sup}(x, y)$ for the larger of x and y . Then for the range of Z we have

$$\text{Min}(Z) = \text{Sup}(0, k + l - n), \quad (28)$$

$$\text{Max}(Z) = \text{Inf}(k, l). \quad (29)$$

To determine the range of D we have to subtract $k \cdot l/n$ from Z , i.e.

$$\text{Min}(D) = \text{Sup}(0, k + l - n) - k \cdot l/n, \quad (30)$$

$$\text{Max}(D) = \text{Inf}(k, l) - k \cdot l/n. \quad (31)$$

Let us assume that $k \leq l$ and that $k + l \leq n$. Then the asymmetry is:

$$a = \frac{n-l}{l} = \frac{1-\lambda}{\lambda} \quad (32)$$

and for $k + l \geq n$ we have:

$$a = \frac{k}{n-k} = \frac{\kappa}{1-\kappa}. \quad (33)$$

For the experimentally relevant parameter range, we always have $k + l \leq n$. According to (32) this means that for firing rates below 10% the asymmetry is larger than $0.9/0.1 = 9$. The asymmetry of sensitivities for excitatory and inhibitory interactions for the normal experimental situation thus is quite large indeed.

5 Discussion

In this paper we have examined the (delayed) coincidence counts between the firings of two simultaneously recorded neurons as expressed in the (normalized) Joint Peri Stimulus Time Histogram. This is usually expressed as a matrix of values, where each entry (bin) corresponds to a particular pair of time delays of the two neurons with respect to a stimulus time marker. We have derived analytic expressions for the probability density of such coincidence counts, under the null hypothesis of independent neurons with the observed individual PST histograms.

These results allow the evaluation of the coincidence probability densities after various normalization procedures that have previously been introduced

in the literature. For each of the normalized correlation measures we have given explicit expressions for the probability density, and from it, the expected value and variance at each bin. The corresponding distributions are non-Gaussian, and have an asymmetric shape and range of values. With physiologically reasonable counts, this asymmetry implies, as has previously been shown, that inhibitory processes are harder to detect than excitatory processes. The given distributions provide the necessary framework for formal evaluation of significance in observed deviations of the coincidence counts from values predicted under the null hypothesis. This is a completely model free approach which results only in a positive or negative statement about the validity of the null hypothesis. Later steps in the analysis process may require the invocation of specific models of neuronal interaction in order to quantify "connectivity" among the neurons (Aertsen et al. 1988).

5.1 Display of Significance Values: Surprise

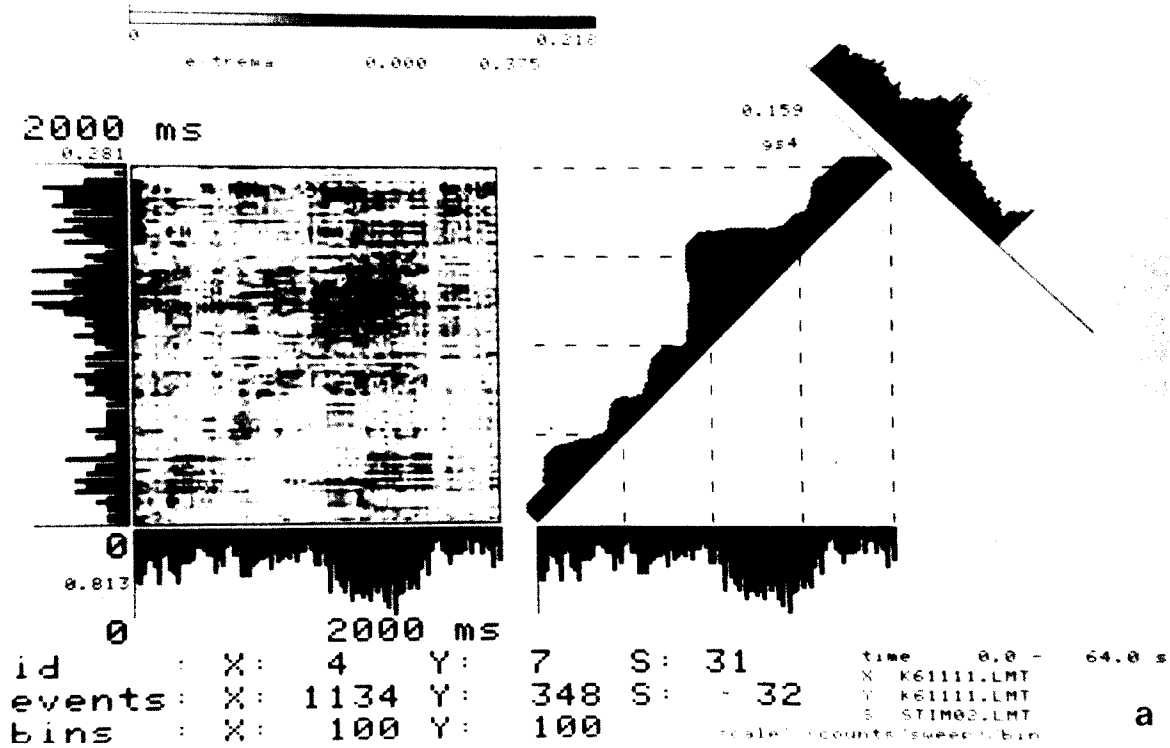
The usual application of significance testing is to state the probability with which the actual observation could occur under the null hypothesis ($p = 0.05$ or 0.01 , for example). The significance value for a given count can be read directly from the graph of the (cumulative) distribution function (cf. Sect. 2.3). However, since we are interested in very small values of the probability, it is appropriate to introduce a logarithmic scale for a more effective display of this graph. Thus, instead of plotting the direct distribution, we will use its negative logarithm; this has been called *entropy* (e.g. Boltzmann 1887; Shannon 1948; Billingsley 1965) or *surprise* (Legéndy 1975; Palm 1981, 1988). The correspondence between the usual significance statement and the surprise measure is a straightforward scale transformation: for example $p = 0.05$ corresponds to a surprise value of 2.996 [i.e. $-\ln(0.05)$]; $p = 0.01$ means a surprise of 4.605.

5.2 Extension of the Surprise to Events in Several Bins

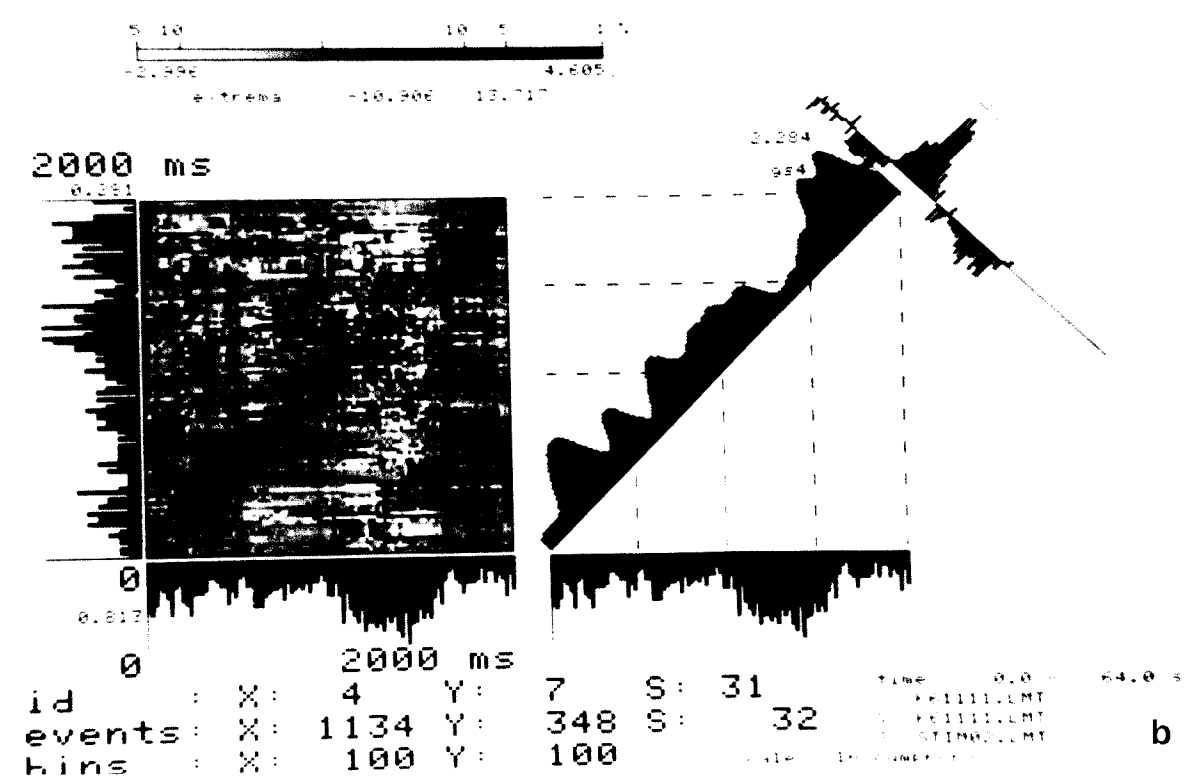
Everything in this paper has so far been based on counts in a single bin. As noted earlier, each such bin corresponds to a particular choice of time delays in the

Fig. 5a and b. Correlation of firing activity among two neurons in the cat's visual cortex (area 17) during stimulation with moving bars (Krüger 1982). **a** Joint PST histogram. *Left:* Matrix of "raw" coincidence counts Z , divided by the number of stimulus presentations n ; values coded according to grey scale above, together with both single unit PST histograms (along abscissa and ordinate); *right:* histogram representation of values in narrow band along main diagonal of JPSTH (time course of near-coincident firing), and time average of near-coincident firing as a function of relative time delay (upper right histogram across diagonal, obtained by integrating JPSTH along diagonal (comparable to normal cross correlogram)). **b** Significance of correlation: difference between surprise for "excitation" and surprise for "inhibition" (display format of **b** as in **a**). Further explanation of the surprise measure is given in the text. [See Aertsen et al. (1988) for a more elaborate discussion on this type of analysis and figures]

Joint-PSTH



Surprise(E) - Surprise(I)



firings of the two neurons with respect to a stimulus marker. Normally, however, we are interested in the complete matrix of such bins; with reasonable choice of time resolution our attention is drawn to coherent deviant regions (“features”) in such a matrix (for an example see Fig. 5).

Figure 5 is obtained from spike sequences, simultaneously recorded from two neurons in the cat’s visual cortex (area 17) during stimulation with moving bars (Krüger 1982). Each bin in the matrices corresponds to the coincidence counts between spikes in a particular pair of time bins, one for each neuron. Figure 5a displays the “raw” coincidence counts Z ; Figure 5b displays the difference between the surprise for “excitation” and the surprise for “inhibition”. Both surprise values are calculated from the cumulative distribution obtained from (7), evaluated for the observed counts of X , Y , and Z at each pair of bins. [For a more comprehensive discussion on the use of such matrices and their interpretation, the reader is referred to Aertsen et al. (1988).] In Fig. 5b we note a distinct, broad region of high surprise values along the main diagonal; this is certainly a more “significant” feature than any of the isolated high surprise values, scattered throughout the matrix.

From this viewpoint, isolated bins which show highly significant deviations in the statistical sense, are of less interest. If we require significant deviation over some contiguous region of bins, we are in effect imposing an extended requirement on significance. (compare Palm 1988). Here we can make use of another property of the surprise measure: it makes sense to add the surprise values of different observations, because surprise is a logarithmic measure of improbability. In our case this implies that we can simply add the surprise values of individual bin counts. Such an integration is, of course, also a smoothing process applied to the surprise matrix. Automatic detection of deviant features in the matrix could utilize algorithms similar to those used for the detection of surprising bursts of firing in the spike trains of neurons (Legéndy and Salcman 1985): starting from a bin with high surprise value, one keeps adding adjacent bins which do not lower the average surprise over the combined area.

5.3 Comparison of the Various Measures of Correlation in Models and Experiments

Several normalised correlation measures were defined in (14)–(18). Studies with spike trains originating from simulated neuronal circuits show that normalizations C (and S) are the most appropriate, in the sense that they most directly allow recovery of the underlying circuit from the correlation measures (Aertsen et al. 1988). The standardized correlation S differs from the

normalized correlation C only by a factor containing the number of sweeps: $\sqrt{(n-1)}$ [cf. (18)].

S has a fixed variance of 1, and, as a consequence, a variable range of values which depends on the number of stimulus presentations. We prefer the correlation measure C , since its values are normalized to the fixed range $[-1, 1]$; this makes comparison across experiments relatively straightforward.

In Fig. 4 we have shown that the coincidence count distribution deviates from Gaussian. However, since in the typical experimental situation these deviations are not dramatic, it is appropriate to examine the applicability of a Gaussian distribution for significance testing. The obvious advantage would be that one can work with the variance alone, rather than with the complete distribution. The necessary variance in this case would be computed in the usual manner, i.e. by averaging the appropriate squared difference over all stimulus presentations. Therefore in this situation we are computing the variance of the coincidence count only over the current realization of the experiment. In contrast, the distributions we have derived in this paper refer to the ensemble of all possible realizations of the coincidence counts under the null hypothesis. Clearly the Gaussian approximation is a more restricted measure, and hence, perhaps to be avoided for these purposes.

The theoretical results given in this paper have been applied in the analysis of correlation of firing in both simulated and physiological spike trains. Such analyses and discussion of their interpretations can be found in (Aertsen et al. 1988; Gerstein 1987; Gerstein et al. 1988). These studies of correlation in multi-neuron firing show that – over a wide range of preparations (both animals and brain areas) – neuronal assembly organization is dynamic on several time scales (milliseconds to seconds), and depends on both stimulus and context.

Acknowledgements. GLG is grateful to Prof. V. Braitenberg for the opportunity of a sabbatical stay at the MPI for Biological Cybernetics during 1986–87. The spike train data for Fig. 5 were kindly provided by Jürgen Krüger. We thank Volker Staiger for skillful assistance in generating the figures.

References

- Abeles M (1982) Local cortical circuits. Studies of brain function, vol 6. Springer, Berlin Heidelberg New York
- Aertsen AMHJ, Gerstein GL (1985) Evaluation of neuronal connectivity: sensitivity of cross correlation. *Brain Res* 340:341–354
- Aertsen A, Bonhoeffer T, Krüger J (1987) Coherent activity in neuronal populations: analysis and interpretation. In: Caianiello ER (ed) *Physics of cognitive processes*. World Scientific Publishing, Singapore, pp 1–34

- Aertsen AMHJ, Gerstein GL, Habib M, Palm G et al. (1988) Dynamics of neuronal firing correlation: modulation of "effective connectivity" (submitted for publication)
- Billingsley P (1965) Ergodic theory and information. Wiley, New York
- Boltzmann L (1887) Über die mechanischen Analogien des zweiten Hauptsatzes der Thermodynamik. *J Reine Angew Math* 100:201–212
- Boogaard H van den, Hesselmann G, Johannesma P (1986) System identification based on point processes and correlation densities. I. The nonrefractory neuron model. *Math Biosci* 80:143–171
- Gerstein G (1987) Information flow and state in cortical neural networks: interpreting multi-neuron experiments. In: Seelen W von, Shaw G, Leinhos U (eds) *Organization of neural networks: structures and models*. VCH Verlagsgesellschaft, Weinheim, pp 53–75
- Gerstein GL, Perkel DH (1969) Simultaneously recorded trains of action potentials: analysis and functional interpretation. *Science* 164:828–830
- Gerstein GL, Perkel DH (1972) Mutual temporal relationships among neuronal spike trains. *Biophys J* 12:453–473
- Gerstein G, Bloom M, Espinosa I, Evanczuk S, Turner M (1983) Design of a laboratory for multi-neuron studies. *IEEE Trans SMC-13*:668–676
- Gerstein GL, Aertsen AMHJ et al. (1988) Neuronal assemblies as observed in multi-neuron experiments: dynamic organization depending on stimulus (in preparation)
- Glaser EM, Ruchkin DS (1976) Principles of neurobiological signal analysis. Academic Press, New York
- Grinvald A (1985) Real-time optical mapping of neuronal activity: from single growth cones to the intact mammalian brain. *Ann Rev Neurosci* 8:263–305
- Habib MK, Sen PK (1985) Non-stationary stochastic point-process models in neurophysiology with applications to learning. In: Sen PK (ed) *Biostatistics: statistics in biomedical, public health and environmental sciences*. Elsevier/North-Holland, Amsterdam, pp 481–509
- Krüger J (1982) A 12-fold microelectrode for recording from vertically aligned cortical neurons. *J Neurosci Methods* 6:347–350
- Krüger J (1983) Simultaneous individual recordings from many cerebral neurons: techniques and results. *Rev Physiol Biochem Pharmacol* 98:177–233
- Kuznetsov PI, Stratonovich RL (1956) A note on the mathematical theory of correlated random points. *Izv Akad Nauk SSSR Ser Math* 20:167–178; also in: Kuznetsov PI, Stratonovich RL, Tikhonov VI (eds) (1965) *Nonlinear transformations of stochastic processes*. Pergamon Press, New York, pp 101–115
- Legény CR (1975) Three principles of brain function and structure. *Int J Neurosci* 6:237–254
- Legény CR, Salzman M (1985) Bursts and recurrences of bursts in the spike trains of spontaneously active striate cortex neurons. *J Neurophys* 53:926–939
- Palm G (1981) Evidence, information, and surprise. *Biol Cybern* 42:57–68
- Palm G (1988) *Information theory*. MIT Press, Cambridge, Mass (in press)
- Perkel DH, Gerstein GL, Moore GP (1967) Neuronal spike trains and stochastic point processes. II. Simultaneous spike trains. *Biophys J* 7:419–440
- Perkel DH, Gerstein GL, Smith MS, Tatton WG (1975) Nerve-impulse patterns: a quantitative display technique for three neurons. *Brain Res* 100:271–296
- Shannon C (1948) A mathematical theory of communication. *Bell Syst Techn J* 27:379–423, 623–656

Received: November 11, 1987

Dr. Ad M. H. J. Aertsen
Max-Planck-Institut für
Biologische Kybernetik
Spemannstrasse 38
D-7400 Tübingen
Federal Republic of Germany